Flight dynamics of boomerangs

Nicklas Jävergård

January 29, 2018

Abstract

In this body of work a paper called ”Boomerang Flight Dynamics” written by John C. Vassberg in 2012 have been thoroughly studied. The goal of this paper were to understand and explain the steps that were omitted in the original paper and clarify some reasoning that leads to conclusions that the original author drew whilst still presenting some of the results and conclusions, perhaps in a different way. A small section of some terminology and basics of aerodynamics was added in order to facilitate understanding of Blade Element Theory later on. The original paper presents a new aerodynamic model that represented a significant advancement in boomerang study. For this paper we arrive in understanding how the aerodynamic forces and moments together with gyroscopic properties combine to determine the dynamic stability and trim that the boomerang exhibits.

Contents

1 Introduction

The paper is made as one of the examining assignments of the classical mechanics course at Karlstads university. The initial goal was to remove approximations made in [2] one by one in order to see what new information this would yield. My goal turned out to be insurmountable so it was reformulated into understanding and explaining the original paper and presenting some significant results.
Describing the flight dynamics of boomerangs is a complex endeavour since it combines mechanical knowledge with the understanding of aero and gyroscope dynamics. In this paper Blade Element Theory(BET) coupled with the Euler equations of motion was used to explain why a boomerang flies in the way that it does.

The throwing-stick type weapons have been used at some point in history by every culture around the globe. They exhibit aero-dynamical properties that extend the range and improve accuracy of the throw. It was only the Australian Aborigines that created the famous returning boomerang. It was used for hunting fowl, by throwing it over some grassing birds and being misinterpreted as a bird of prey causing the birds to fly low and thus facilitated the capture of said fowl. The boomerang was also used just like today for recreation and sports.

Boomerangs look deceptively simple. However, their dynamics are indeed complex. Rotation causes the airflow over any surface to be three dimensional and it reverses in such a way that the leading and trailing edges of the boomerang swap roles twice every revolution. The rotation also give rise to a differential relative airspeed between the forward and backward moving blade. This difference in airspeed translates into a proportional offset in the forces generated.

A boomerang in mid flight is constantly changing its orientation to any external reference system therefore an detailed explanation of Euler angles will follow in order to allow understanding of the kinematics governing boomerang flight.

2 Euler angles

In Figure 1 the inertial frame is given by $\hat{x}', \hat{y}'\hat{z}'$ and the body frame by $\hat{x}, \hat{y}, \hat{z}$ The angles ϕ, ψ, θ have been used to transform between the inertial and body frame. This procedure is rather straight forward. The first rotation is about the $\hat{z}'$-axis through and angle ϕ and results in two new axes in the $\hat{x}'$ and $\hat{y}'$ plane. In Figure 1 only the new $\hat{x}'$-axis is shown and is denoted $\hat{n}$. The rotation is represented by the matrix, $\boldsymbol{A}$.

$$\boldsymbol{A} = \begin{bmatrix} \cos(\phi) & \sin(\phi) & 0 \\ -\sin(\phi) & \cos(\phi) & 0 \\ 0 & 0 & 1 \end{bmatrix}$$

Figure 1: The orientation angles ϕ, ψ, θ to transform the inertial into the body system

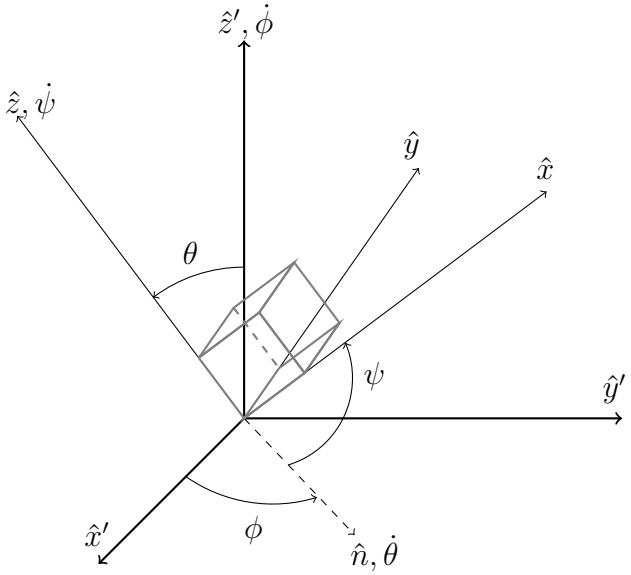

The second rotation is about the $\hat{n}$-axis through and angle θ this fixates the $\hat{z}$-axis in the body system. This is done by matrix $\boldsymbol{B}$

$$\boldsymbol{B} = \begin{bmatrix} 1 & 0 & 0 \\ 0 & \cos(\theta) & \sin(\theta) \\ 0 & -\sin(\theta) & \cos(\theta) \end{bmatrix}$$

The final rotation takes place through an angle ψ about the body frame $\hat{z}$-axis which fixates both the $\hat{x}$ and $\hat{y}$-axes in the body system. The last rotation is given below:

$$\boldsymbol{C} = \begin{bmatrix} \cos(\psi) & \sin(\psi) & 0 \\ -\sin(\psi) & \cos(\psi) & 0 \\ 0 & 0 & 1 \end{bmatrix} \tag{1}$$

These three rotations together describe the orientation of the boomerang as it flies through the air. $\dot{\psi}$,$\dot{\theta}$ and $\dot{\phi}$ describe the rotational speed about its centre of mass, the change in angle of bank and the precession about the vertical axis in the inertial frame, respectively. The convention used here to describe the transformation is called the zxz convention, that is to specify about which axis the rotations are made and in what order. It should be added for clarity that any three rotations about different axes could have been used to describe the orientation however with these three is becomes especially easy to say what the different rotations represent. Let X' be a matrix that specifies the inertial frame. If $\boldsymbol{A}$ represents the first rotation and $\boldsymbol{B}$, $\boldsymbol{C}$ the consecutive ones in order of application the transformation

can be represented as follows.

$$X = \boldsymbol{CBA}X'$$

$\boldsymbol{CBA}$ can also be multiplied together in order to represent the entire transformation using a single matrix. This is given below, where c and s represents cosine and sine respectively.

$$\boldsymbol{T}^{x'x} = \begin{bmatrix} c\phi c\psi - s\phi c\theta s\psi & s\phi c\psi + c\phi c\theta s\psi & s\theta s\psi \\ -c\phi s\psi - s\phi c\theta c\psi & -s\phi s\psi + c\phi c\theta c\psi & s\theta c\psi \\ s\phi s\theta & -c\phi s\theta & c\theta \end{bmatrix}$$

$\boldsymbol{T}^{x'x}$ represents the transformation from the inertial system to the body system, since this is pure rotational the inverse $\boldsymbol{T}^{xx'}$ would simply be the transpose of $\boldsymbol{T}^{x'x}$

3 Euler equations of angular motion

The general Euler equations of motion is given below.

$$M_x = I_{xx}\dot{\omega}_x + \Big(I_{zz} - I_{yy}\Big)\omega_y\omega_z \tag{2a}$$

$$M_y = I_{yy}\dot{\omega}_y + \Big(I_{xx} - I_{zz}\Big)\omega_x\omega_z \tag{2b}$$

$$M_z = I_{zz}\dot{\omega}_z + \Big(I_{yy} - I_{xx}\Big)\omega_x\omega_y \tag{2c}$$

These equations are in the principal axis frame of the body system described by $\hat{x}, \hat{y}$ and $\hat{z}$. Fortunately these axes coincide with the appropriate directions for describing the boomerang, otherwise the equations would be a lot more complicated. The z-axis is the axis of rotation and the x-direction is the direction of air flow leaving the y-axis to be along the wingspan. Since the equations are describing the body system another set of equations are needed to relate the ω's to the Euler angles of rotation. In order to derive these a second look at the transformations matrices are needed. The first angular velocity that needs to be transformed is $\dot{\phi}$. Since this angular velocity is about an axis in the inertial frame($\hat{z}'$), it needs to be transformed using $\boldsymbol{T}^{x'x}$ which transforms from inertial to body system. The transformation is carried out below.

$$\begin{bmatrix} c\phi c\psi - s\phi c\theta s\psi & s\phi c\psi + c\phi c\theta s\psi & s\theta s\psi \\ -c\phi s\psi - s\phi c\theta c\psi & -s\phi s\psi + c\phi c\theta c\psi & s\theta c\psi \\ s\phi s\theta & -c\phi s\theta & c\theta \end{bmatrix} \begin{bmatrix} 0 \\ 0 \\ \dot{\phi} \end{bmatrix} = \begin{bmatrix} \dot{\phi}\sin(\theta)\sin(\psi) \\ \dot{\phi}\sin(\theta)\cos(\psi) \\ \dot{\phi}\cos(\theta) \end{bmatrix} \tag{3}$$

Now the second angular velocity that needs to be transformed into the body system is $\dot{\theta}$. In order for this angular velocity to be aligned with the body system, only one

rotation is needed. The rotation through the angle ψ. This is the transformation given by $\boldsymbol{C}$. Another thing that needs to be remembered: $\dot{\theta}$ is along the $\hat{n}$-axis however in this "intermediate" step in the transform the $\hat{n}$-axis can be thought of as a "new" x-axis. This will help us write the angular velocity vector in the correct manner.

$$\begin{bmatrix} \cos(\psi) & \sin(\psi) & 0 \\ -\sin(\psi) & \cos(\psi) & 0 \\ 0 & 0 & 1 \end{bmatrix} \begin{bmatrix} \dot{\theta} \\ 0 \\ 0 \end{bmatrix} = \begin{bmatrix} \dot{\theta}\cos(\psi) \\ -\dot{\theta}\sin(\psi) \\ 0 \end{bmatrix} \tag{4}$$

The last angular velocity($\dot{\psi}$) does not require a transform, since that rotation is about the $\hat{z}$-axis in the body system. To obtain equations that connect the ω's and Euler angles, one simply add up the components from the transforms. If this is done, the equations below are obtained:

$$\omega_x = \dot{\phi}\sin(\theta)\sin(\psi) + \dot{\theta}\cos(\psi), \tag{5a}$$

$$\omega_y = \dot{\phi}\sin(\theta)\cos(\psi) - \dot{\theta}\sin(\psi), \tag{5b}$$

$$\omega_z = \dot{\psi} + \dot{\phi}\cos(\theta). \tag{5c}$$

If the equations represented in 5 are differentiated with respect to time, the $\dot{\omega}'$s are determined:

$$\dot{\omega}_x = \ddot{\phi}\sin(\theta)\sin(\psi) + \dot{\phi}\dot{\theta}\cos(\theta)\sin(\psi) + \dot{\phi}\dot{\psi}\sin(\theta)\cos(\psi) + \ddot{\theta}\cos(\psi) - \dot{\theta}\dot{\psi}\sin(\psi), \tag{6a}$$

$$\dot{\omega}_y = \ddot{\phi}\sin(\theta)\cos(\psi) + \dot{\phi}\dot{\theta}\cos(\theta)\cos(\psi) - \dot{\phi}\dot{\psi}\sin(\theta)\sin(\psi) - \ddot{\theta}\sin(\psi) - \dot{\theta}\dot{\psi}\cos(\psi), \tag{6b}$$

$$\dot{\omega}_z = \ddot{\psi} + \ddot{\phi}\cos(\theta) - \dot{\phi}\dot{\theta}\sin(\theta). \tag{6c}$$

From these derivatives it is plain to see that the equations of motion once equations 5 and 6 are inserted into 2 wont be easily solved. However there is some instructional value in doing so anyway.

$$\begin{aligned} M_x &= I_{xx}\Big(\ddot{\phi}\sin(\theta)\sin(\psi) + \dot{\phi}\dot{\theta}\cos(\theta)\sin(\psi) + \dot{\phi}\dot{\psi}\sin(\theta)\cos(\psi) + \ddot{\theta}\cos(\psi) - \dot{\theta}\dot{\psi}\sin(\psi)\Big) \\ &\quad + \Big(I_{zz} - I_{yy}\Big)\Big(\dot{\phi}\dot{\psi}\sin(\theta)\cos(\psi) + \dot{\phi}^2\sin(\theta)\cos(\theta)\cos(\psi) - \dot{\theta}\dot{\psi}\sin(\psi) - \dot{\phi}\dot{\theta}\dot{\psi}\cos(\theta)\sin(\psi)\Big) \\ M_y &= I_{yy}\Big(\ddot{\phi}\sin(\theta)\cos(\psi) + \dot{\phi}\dot{\theta}\cos(\theta)\cos(\psi) - \dot{\phi}\dot{\psi}\sin(\theta)\sin(\psi) - \ddot{\theta}\sin(\psi) - \dot{\theta}\cos(\psi)\Big) \\ &\quad + (I_{xx} - I_{zz})\Big(\dot{\phi}\dot{\psi}\sin(\theta)\sin(\psi) + \dot{\phi}^2\sin(\theta)\cos(\theta)\sin(\psi) + \dot{\theta}\dot{\psi}\cos(\psi) + \dot{\phi}\dot{\theta}\cos(\theta)\cos(\psi)\Big) \\ M_z &= I_{zz}\Big(\ddot{\psi} + \ddot{\phi}\cos(\theta) - \dot{\phi}\dot{\theta}\sin(\theta)\Big) \\ &\quad + (I_{yy} - I_{xx})\Big(\dot{\phi}^2\sin^2(\theta)\sin(\psi)\cos(\psi) - \dot{\phi}\dot{\theta}\sin(\theta)\sin^2(\psi) + \dot{\phi}\dot{\theta}\sin(\theta)\cos^2(\psi) - \dot{\theta}^2\sin(\psi)\cos(\psi)\Big) \end{aligned} \tag{7}$$

If the inertial moments I_{xx} and I_{yy} would be equal the expression for M_z would be greatly simplified and would facilitate further simplifications of M_x and M_y since they are similar. For a static boomerang there is no way the moments about $\hat{x}$ and $\hat{y}$ would be equal, however since the boomerang rotates as it flies through the air the mass distribution could be averaged over one revolution and the inertial moments would be equal as a result. After that simplification the focus now lies on M_x and M_y. In every term the difference between M_x and M_y is that in one it contains a $\cos(\psi)$ factor and in the other a $\sin(\psi)$ factor. This suggests that if they were projected on different axes the equations of motion would simplify. The appropriate axes are presented below.

$$\hat{n} = \cos(\psi)\hat{x} - \sin(\psi)\hat{y} \tag{8}$$

with $\hat{s}$ perpendicular to $\hat{n}$, but in the same plane.

$$\hat{s} = \sin(\psi)\hat{x} + \cos(\psi)\hat{y} \tag{9}$$

When determining the moment about the $\hat{n}$-axis there will be an overall cosine on M_x and a -sine on M_y. For the moment about $\hat{s}$ axes, the projection will be the same up to a minus sign on the sine term.
The inertial moment simplification results in $I_{xx} = I_{yy} \equiv I_{rr}$. What effects other then simplifying the equations of motion would this entail?

The high frequency dynamics of boomerangs is lost from the model. Since the mass distribution is averaged over one revolution no specific dynamical events within one revolution can be isolated, therefore conclusions draw about the dynamics within one revolution will be very uncertain if any are possible. The good news is the low frequency dynamics will be retained and, even with an accurate inertial description, the stability of the boomerang would still largely depend upon the average forces and moments. The simplified equations of motion are given below:

$$M_n = I_{rr}\ddot{\theta} + (I_{zz} - I_{rr})\dot{\phi}^2 \sin(\theta)\cos(\theta) + I_{zz}\dot{\phi}\dot{\psi}\sin(\theta), \tag{10a}$$

$$M_s = I_{rr}\Big(\ddot{\phi}\sin(\theta) + 2\dot{\theta}\dot{\phi}\cos(\theta)\Big) - I_{zz}\dot{\theta}(\dot{\psi} + \dot{\phi}\cos(\theta)), \tag{10b}$$

$$M_z = I_{zz}\left(\ddot{\psi} + \ddot{\phi}\cos(\theta) - \dot{\phi}\dot{\theta}\sin(\theta)\right). \tag{10c}$$

Further simplifications of the expression are possible by inserting the simplified moments of inertia:

$$I_{zz} = \frac{1}{2}mR^2 = 2I_{rr}, \tag{11}$$

where m is the mass of the boomerang and R it's radius as in Figure 2. If the moment of inertia is inserted into 10 the below result is obtained:

Figure 2: Modified picture of a boomerang, displaying its radius and chord length [1]

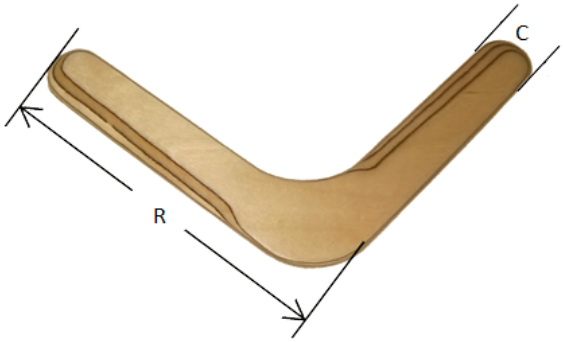

$$
\begin{aligned}
M_n &= \frac{1}{4}mR^2\Big(\ddot{\theta} + \dot{\phi}^2\sin(\theta)\cos(\theta) + 2\dot{\phi}\dot{\psi}\sin(\theta\Big),\\
M_s &= \frac{1}{4}mR^2\Big(\ddot{\phi}\sin(\theta) - 2\dot{\theta}\dot{\psi}\Big),\\
M_z &= \frac{1}{2}mR^2\Big(\ddot{\psi} + \ddot{\phi}\cos(\theta) - \dot{\phi}\dot{\theta}\sin(\theta)\Big).
\end{aligned}
$$

From this point going forward, a case where the rolling moment is purely about the $\hat{n}$ will be looked at. This would result in M_s being equal to zero since it is in the same plane as M_n. Furthermore lets assume that θ is constant, meaning the first and second derivatives are zero. These assumption would leave us with the same equations governing a symmetrical heavy top with one point kept fixed. The equations are stated below:

$$
\begin{aligned}
M_n &= \frac{1}{4}mR^2\Big(\dot{\phi}^2\sin(\theta)\cos(\theta) + 2\dot{\phi}\dot{\psi}\sin(\theta)\Big),\\
0 &= \ddot{\phi},\\
0 &= \ddot{\psi}.
\end{aligned}
$$

From the above equations one can read that the top would rotate about its own axis at a constant $\dot{\psi}$ with a constant precession rate $\dot{\phi}$ about the inertial frame $\hat{z}'$-axis. The moment that governs the precession of the top originates from the force due to gravity and the lateral distance between the pivot point and centre of mass. In the boomerang case the same moment would be provided by aerodynamic forces. The forces and resulting moments will be calculated/presented and explained in the Basic aerodynamic and Blade Element Theory sections.

4 Kinematics of boomerang flight

This section is a representation of the experimental data obtained in [2] where the author determines the initial conditions and bounding values for a boomerang throw. Imagine firstly that a ball is rolling without slipping on the floor. The ball translational velocity is connected to its angular velocity according to $\omega R = V$. Now imagine that a ball is rolling off your hand without slipping. Whilst in the air, the same condition still applies. In [2] a similar expression was derived experimentally for the throwing of boomerangs.

$$V_0 = 0,85\omega_0 R$$

The numerical factor of 0.85 in the formula seems to be due to the fact that the blade needs to be held firmly during the throw. This results in the boomerang being unable to roll through the hand as easily. The data is confirmed by the analysis of a boomerang with LEDs at the wing tip thrown in darkness. Later it in [2] it is stated that a boomerang requires a minimum value of $\chi_0 = \frac{\omega_0 R}{V_0} = 0.7$ in order to achieve stable flight. This ratio is called the tip speed ratio and the initial value as stated must be larger then 0.7. This factor increases during flight because the translational speed reduces faster then the rotational speed. Therefore a new variable is introduced.

$$\chi = \frac{\omega R}{V} \tag{12}$$

The angle from the horizontal at the point of release is given the Euler angle θ_0

$$70^\circ \leq \theta_0 \leq 80^\circ$$

5 Basic aerodynamics

Figure 3: Terms and shape of an air-foil [3][This figure has been modified from the original]

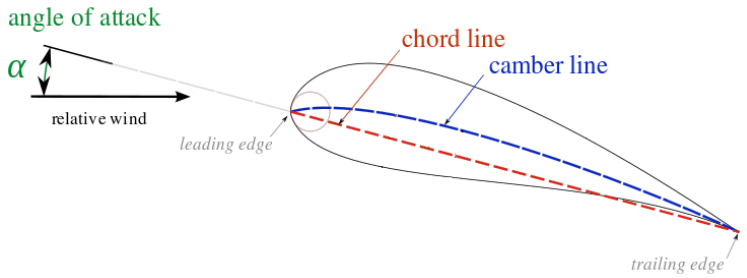

Figure 3 shows some of the terminology needed to describe an air-foil and also the shape of a generic air-foil. The chord line is a straight line joining the trailing and leading edge of the wing and the angle between the extension of this line and the relative wind velocity is the angle of attack given by α. This is a very important parameter when discussing the aerodynamics of any air-foil since it is the parameter that can be influenced the easiest during flight, intentionally or unintentionally. The camber line is a line joining the leading and trailing edge of the wing that is equidistant from the upper and lower surface. A wing is said to have positive camber if the camber line is always above the chord line and this is a measure of the curvature of the wing. An important aspect to keep straight is that if an air-foil has a positive camber it will generate lift, even if the angle of attack is zero or perhaps negative. With this said, lets take a look at a simple model of aerodynamic forces, lift in particular:

$$F_{lift} = \frac{1}{2} C_l \rho A V^2,$$

C_l = coefficient of lift,

ρ = air density,

A = Plan form area of the wing,

V = Air speed of the airflow relative to the wing.

The area of a wing for the boomerang will henceforth be described as chord length times radius (CR). The coefficient of lift depends on a lot of complex things such as the three dimensional airflow, vortex formation, aspects of interference between different surfaces and so on. However for the purposes in this paper a simplification is made where the coefficient is a linear function that depends on α. Before it is possible to discuss the intricacies of boomerang aerodynamics, a basic understanding of how any aerodynamic force(including lift) is generated. Imagine two separate particles approaching the air-foil in Figure 3. The particles get separated by the wing with one flowing above and the other underneath. Due to the Coanda effect[4] both particles will have a tendency to follow the shape of the wing. As the particles leave the trailing edge of the wing their velocity has changed in direction and possibly in magnitude. However it is the change in direction that is important. The airflow has this way been deflected downward after the wing and according to Newtons third law of motion, if the air is accelerated downward the wing must be accelerated upward and this is the origin of the lifting force. In the next section Blade Element Theory will be used to calculate the forces and moments governing the boomerang.

6 Blade element theory

Blade Element Theory is a mathematical process devised to calculate the thrust generated by propellers[5]. Thrust is the forward force generated by air being accelerated backwards by the propellers. Blade element theory is a convenient model to use since a propeller is a set of rotating wings and a boomerang is essentially the same thing. The moments and forces are calculated by determining the contribution of a differential area and integrating over the entire blade and averaged over one complete revolution. The major difficulty in this theory is in providing an accurate model of the airflow. In "Boomerang Flight Dynamics" [2] a simple model for the airflow was used to determine the forces and moments. Since a small angles approximation is used for the angle of attack one can split the coefficient of lift in to two parts as shown in 13.

$$C_l(\alpha) = C_{l0} + \alpha C_{l\alpha} \tag{13}$$

Where C_{l0} and $C_{l\alpha}$ are constants.

In order to calculate the forces and moments a representation of the differential elements of integration is needed. This is given in Figure 4.

Figure 4: Schematic of a non-tapered boomerang blade in flight as seen from above

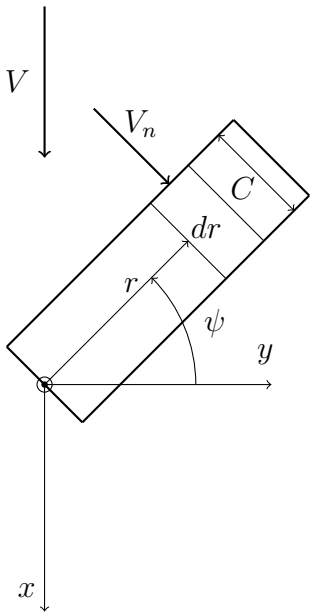

In Figure 4 the labels mean the following:

V - Free stream velocity of the airflow.

V_n - Perpendicular velocity of the airflow

r - Length along the blade to reach the differential element dr

C - Chord length

ψ - Angular position of the blade, $0 < \psi < 2\pi$

In order to get a comprehensive model of the blades as they rotate during flight, the lift force, rolling and the pitching moment needs to be calculated. This is a laborious process with the same tactics for each of these, therefore only the lift derivation will be presented here. If the reader is interested the entire derivation is presented in [2]. Before this can be done, an approximate model of the airflow is needed. The forces and moments will be calculated using two dimensional airflow and this will lead to the conclusion that only the airflow perpendicular to the wing will be relevant. By looking at Figure 4 one can determine that

$$V_n(r, \psi) = V \cos(\psi) + \dot{\psi} r \tag{14}$$

The blade "cuts" the air with an angle α, this must mean that there is a z-component to the velocity vector.

$$V_z = V \sin(\alpha) \approx \alpha V \tag{15}$$

Where the later part of equation 15 can be used, since small angles of attack are considered. As the blade rotates through the angle ψ the airflow reverses and thus both V_n and α goes through a cyclic change for each revolution. To understand this cyclic change, keep in mind that the magnitude of the perpendicular airspeed will depend upon the orientation of the blade. Therefore an effective angle of attack α_e is introduced:

$$\alpha_e = \tan^{-1}\left(\frac{V_z}{|V_n|}\right) \approx \frac{V_z}{|V_n|}, \tag{16}$$

The absolute value is explained by the fact that the airflow reverses twice during one revolution but the effective angle of attack should be dependent only on the sign of V_z. That concludes this simple model of the relative airflow. If we set the maximal radius of the boomerang to R we end up with the following expression for the lift that is present with $\alpha = 0$

$$L_0(\psi) = \int_0^R \frac{1}{2} C C_{l0} \rho V_n^2 \, dr$$

By inserting equation 14 we obtain the following expression

$$\begin{aligned} L_0(\psi) &= \frac{1}{2}CC_{l0}\rho\int_0^R \Big(V\cos(\psi)+\dot{\psi}r\Big)^2\,dr = \\ &= \frac{1}{2}CC_{l0}\rho V^2\int_0^R \cos^2(\psi)+\frac{2\dot{\psi}r\cos(\psi)}{V}+\frac{\dot{\psi}^2r^2}{V^2}dr = \\ &= \frac{1}{2}CC_{l0}\rho V^2R\left[\cos^2(\psi)+\frac{\dot{\psi}R\cos(\psi)}{V}+\frac{\dot{\psi}^2R^2}{3V^2}\right] \end{aligned} \tag{17}$$

The expression given in 17 is the lift generated at specific angular positions as a function of ψ. This is then integrated over one revolution and divided by 2π, this yields the average force generated by one revolution. Since the lift is symmetric about the y-axis given in Figure 4 the integration can be performed from 0 to π instead. For ease of notation lets introduce $\chi = \frac{\dot{\psi}R}{V}$ which is a nondimensionalized form of the rotational speed or the ratio between the tip speed of the blade and the translational speed of the body as discussed in the section about kinematics.

$$\begin{aligned} \bar{L}_0 &= \frac{1}{\pi}\int_0^\pi CC_{l0}\rho V^2R\left[\cos^2(\psi)+\chi\cos(\psi)+\frac{\chi^2}{3}\right]d\psi = \\ &= \frac{1}{\pi}CC_{l0}\rho V^2R\left[\frac{1}{2}(\psi+\sin(\psi)\cos(\psi))+\chi\sin(\psi)+\frac{\chi^2}{3}\psi\right]_0^\pi = \\ &= \frac{1}{2}CC_{l0}\rho V^2R\left(\frac{1}{2}+\frac{\chi^2}{3}\right) \end{aligned} \tag{18}$$

$\bar{L}_0$ is the time average lift generated independent of the angle of attack, α. Now the lift due to α needs to be determined.

$$L_\alpha(\psi) = \int_0^R \frac{1}{2}C\alpha_e C_{l\alpha}\rho|V_n|^2\,dr \tag{19}$$

By using the fact that $|V_n|\alpha_e = V_z \approx \alpha V$ and insert the expression for V_n we end up with the following expression.

$$\begin{aligned} L_\alpha(\psi) &= \frac{1}{2}C\rho C_{l\alpha}\alpha V\int_0^R |V\cos(\psi)+\dot{\psi}r|\,dr = \\ &= \frac{1}{2}C\rho C_{l\alpha}\alpha V^2\int_0^R |\cos(\psi)+\chi\Big(\frac{r}{R}\Big)|\,dr = \\ &= \left[\eta=\frac{r}{R}\right] = \frac{1}{2}C\rho C_{l\alpha}\alpha V^2R\int_0^1 \Big|\cos(\psi)+\chi\eta\Big|d\eta \end{aligned} \tag{20}$$

The integrand in equation 20 is a straight line and depending on the angle it will start above or below the y-axis. For a boomerang in mid flight the slope of this

line will always be positive however whether it will be steep enough to cross the y-axis before it reaches $\chi = 1$ is subject to initial conditions of the boomerang as it is being thrown. The result of integrating this line will depend on the value of χ. The case where a straight line starts below some x-axis and ends up above it before $x = 1$ is presented in Figure 5.

Figure 5: Straight line

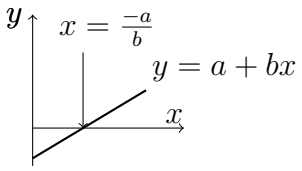

The integration of the absolute value of such a line is determined below.

$$I = \int_0^1 |a + bx| dx = \int_0^{\frac{-a}{b}} -(a + bx)dx + \int_{\frac{-a}{b}}^1 (a + bx)dx = \\ = \frac{a^2}{b} + a + \frac{b}{2} \tag{21}$$

By virtue of 21 the integration in 20 can be readily split into its different cases and calculated easily.
With $0 < \psi < \frac{\pi}{2}$ and $\chi > 0$ the absolute value can be ignored.

$$L_{\alpha 1}(\psi) = \frac{1}{2}\rho V^2 CR\alpha C_{l\alpha}\Big(\cos(\psi) + \frac{\chi}{2}\Big) \tag{22}$$

For the case where $\frac{\pi}{2} < \psi < \pi$ and $\chi > 1$ the result from the general integration formula presented in 21 is used

$$L_{\alpha 2}(\psi) = \frac{1}{2}\rho V^2 CR\alpha C_{l\alpha}\Big(\frac{\cos^2(\psi)}{\chi} + \cos(\psi) + \frac{\chi}{2}\Big) \tag{23}$$

in the next case where $\frac{\pi}{2} < \psi < \arccos(-\chi)$ and $\chi < 1$ the integrand in 20 switches sign during integration thus obtaining and identical result as for $L_{\alpha 2}$

$$L_{\alpha 3}(\psi) = \frac{1}{2}\rho V^2 CR\alpha C_{l\alpha}\Big(\frac{\cos^2(\psi)}{\chi} + \cos(\psi) + \frac{\chi}{2}\Big) \tag{24}$$

The final case is when $\arccos(-\chi) < \psi < \pi$ and $\chi < 1$, in this situation the integrand is always negative thus yielding the following result.

$$L_{\alpha 4}(\psi) = \frac{1}{2}\rho V^2 CR\alpha C_{l\alpha}\Big(-\cos(\psi) - \frac{\chi}{2}\Big) \tag{25}$$

With the lift as a function of ψ determined and time-averaged result can be obtained by integrating over one revolution, remembering that lift is symmetric about the y-axis allows for integration from 0 to π. With this integration being separated into two cases it is important to remember that all different values of χ must be integrated over the half circle. This means that there will be a lot of rearranging in order to make it in two cases. The aforementioned cases are $\chi < 1$ and $1 \leq \chi$. Firstly, the case where $1 \leq \chi$ is presented:

$$\begin{aligned}
\bar{L}_{\alpha 1} &= \frac{1}{\pi}\left(\int_0^{\frac{\pi}{2}} L_{\alpha 1}\, d\psi + \int_{\frac{\pi}{2}}^{\pi} L_{\alpha 2}\, d\psi \right) = \\
&= \frac{1}{2}\rho V^2 C R \alpha C_{l\alpha} \frac{1}{\pi}\left(\int_0^{\pi} \left[\cos(\psi) + \frac{\chi}{2} \right] d\psi + \int_{\frac{\pi}{2}}^{\pi} \left[\frac{\cos^2(\psi)}{\chi} \right] d\psi \right) = \\
&= \frac{1}{2}\rho V^2 C R \alpha C_{l\alpha} \frac{1}{\pi}\left(\left[\sin(\psi) + \frac{\chi}{2}\psi \right]_0^{\pi} d\psi + \left[\frac{1}{2\chi}\big(\psi + \sin(\psi)\cos(\psi) \big) \right]_{\frac{\pi}{2}}^{\pi} d\psi \right) = \\
&= \frac{1}{2}\rho V^2 C R \alpha C_{l\alpha} \left(\frac{\chi}{2} + \frac{1}{4\chi} \right) \qquad (26)
\end{aligned}$$

The next integration is performed in much the same way but with an unknown angle, lets call it $\psi_c = \arccos(-\chi)$. For $\chi < 1$:

$$\begin{aligned}
\bar{L}_{\alpha 2} &= \int_0^{\frac{\pi}{2}} L_{\alpha 1}\, d\psi + \int_{\frac{\pi}{2}}^{\psi_c} L_{\alpha 3}\, d\psi + \int_{\psi_c}^{\pi} L_{\alpha 4}\, d\psi = \\
&= \frac{1}{2}\rho V^2 C R \alpha C_{l\alpha} \frac{1}{\pi}\left(\int_0^{\psi_c} \big(\cos(\psi) + \frac{\chi}{2} \big) d\psi + \int_{\frac{\pi}{2}}^{\psi_c} \big(\frac{\cos^2(\psi)}{\chi} \big) d\psi - \int_{\psi_c}^{\pi} \big(\cos(\psi) + \frac{\chi}{2} \big) d\psi \right) = \\
&= \frac{1}{2}\rho V^2 C R \alpha C_{l\alpha} \frac{1}{\pi}\left(\big[\sin(\psi_c) + \frac{\chi\psi_c}{2} \big] + \frac{1}{2\chi}\big[\psi_c + \sin(\psi_c)\cos(\psi_c) - \frac{\pi}{2} \big] - \big[\frac{\chi\pi}{2} - \big(\sin(\psi) + \frac{\chi\psi_c}{2} \big) \right. \\
&= \frac{1}{2}\rho V^2 C R \alpha C_{l\alpha} \frac{1}{\pi}\left(\big(2 + \frac{\cos(\psi_c)}{2\chi} \big) \sin(\psi_c) + \chi(\psi_c - \frac{\pi}{2}) + \frac{1}{2\chi}(\psi_c - \frac{\pi}{2}) \right) \qquad (27)
\end{aligned}$$

In order to simplify, the arccos needs to be expressed as an arcsine. This is done by Figure 6 with $\chi = \frac{\omega R}{V}$ and $\psi_c = \arccos(-\chi)$. With the help of Figure 6 one can rewrite ψ_c in the following manner, $\psi_c = \arcsin(\frac{\sqrt{V^2 - \omega^2 R^2}}{V})$. By inserting this into equation 27, the following expression is obtained:

$$\bar{L}_{\alpha 2} = \frac{1}{2}\rho V^2 C R \alpha C_{l\alpha} \frac{1}{\pi}\left(\frac{3}{2}\sqrt{1 - \chi^2} + (\psi_c - \frac{\pi}{2})\big(\chi + \frac{1}{2\chi} \big) \right). \qquad (28)$$

Now $\bar{L}_{\alpha 1}$ and $\bar{L}_{\alpha 2}$ lift forces are valid for $1 \leq \chi$ and $1 > \chi$ respectively whilst $\bar{L}_0$ is valid for both cases. In order to simplify the last expression a bit, lets recall from

Figure 6: Representative triangle

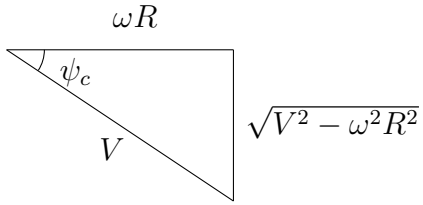

the kinematics section that the value for χ is approximately 0.85 and that it has a lower bound for 0.7. This allow an expansion of ψ_c about $\chi = 1$.

$$\psi_c = \arccos(-\chi) \approx \left(\pi - 2\sqrt{1-\chi}\right) - \frac{1}{6\sqrt{2}\sqrt{1-\chi}^{\frac{3}{2}}} - ... \tag{29}$$

By only using the first term it can be seen that the expression for $\bar{L}_{\alpha 2}$ can be written as follows.

$$\bar{L}_{\alpha 2} \approx \frac{1}{2}\rho V^2 C R \alpha C_{l\alpha}\left(\frac{3}{2\pi}\sqrt{1-\chi^2} + \left(1 - \frac{2\sqrt{2}}{\chi\pi}\sqrt{1-\chi}\right)\left(\frac{\chi}{2} + \frac{1}{4\chi}\right)\right) \tag{30}$$

From equation 26 and 30 it can be observed that the transition for $\chi = 1$ is smooth and thus we may write and expression that is valid for $0.7 \leq \chi$ assuming that the Taylor expansion is accurate enough. Determining the coefficient of total lift by combining 18 26 and 30, and dividing away $\frac{1}{2}\rho V^2 RC$ from the lift formula, denoted $\bar{C}_L$

$$\bar{C}_L \approx C_{l0}\left[\frac{1}{2} + \frac{\chi^2}{3}\right] + \alpha C_{l\alpha}\left(\left[\frac{\chi}{2} + \frac{1}{4\chi}\right]\left[1 - \frac{2\sqrt{2}}{\pi}\sqrt{1-\hat{\chi}}\right] + \frac{3}{2\pi}\sqrt{1-\hat{\chi}^2}\right) \tag{31}$$

where $\hat{\chi} = min(\chi, 1)$ in order to incorporate both derivations in the same formula.

Hopefully this derivation as done in [2] and explained here will be illuminating enough for the moments from roll and pitch to be comprehended. Thus only the results from these calculations will be given below. As a side note it should be mentioned that the coefficients of lift and other forces/moments are derived experimentally and with Computational fluid dynamics(CFD) in [2] but will not be addressed in this paper.

$$\bar{M}_0 = \frac{1}{2}\rho V^2 R^2 C C_{l0}\chi \tag{32a}$$

$$\bar{M}_{\alpha 1} = \frac{1}{2}\rho V^2 R^2 C \alpha C_{l\alpha}\left(\frac{1}{4} - \frac{1}{16\chi^2}\right) \tag{32b}$$

$$\bar{M}_{\alpha 2} = \frac{1}{2} C R^2 \alpha C_{l\alpha} \left(\frac{\pi - 2\psi_c}{16\pi\chi^2} + \frac{\sqrt{1-\chi^2}}{8\pi\chi} - \frac{\pi - 2\psi_c}{4\pi} + \frac{\chi\sqrt{1-\chi^2}}{4\pi} \right) \tag{32c}$$

where the above equations are the rolling moments for zero angle of attack, $1 \leq \chi$ and $\chi < 1$ respectively. Total coefficient for the rolling moment is obtained in a similar fashion as the coefficient of total lift.

$$\bar{C}_M \approx \frac{1}{3} C_{l0} \chi + \alpha C_{l\alpha} \left(\left[\frac{1}{4} - \frac{1}{16\chi^2} \right] \left[1 - \frac{2\sqrt{2}}{\pi} \sqrt{1-\hat{\chi}} \right] + \frac{\sqrt{1-\hat{\chi}^2}}{4\pi} \left(\frac{1}{2\hat{\chi}} + \hat{\chi} \right) \right) \tag{33}$$

where the same conditions apply as did to the coefficient of total lift. The pitching moment for the boomerang are trivial and this is due to the fact that lifting forces in the BET formulation is symmetric about the y-axis. When this is used to calculate the avergare pitching moment we end up with zero.

$$\bar{C}_P = 0 \tag{34}$$

With the lift derived and the tactics for the calculation of the rolling moment using BET laid out it is possible to move on to stability and trim.

7 Static trim and dynamic stability

For the stability and trim of a boomerang the interesting parameter is the angle of attack. Trim angle is the angle α at which the moments that act on the boomerang cannot give rise to a change in α. This is called static trim due to the fact that the trim angle is determined exclusively by design and is not subject to initial conditions. This is closely related to stability. If an object is dynamically stable it means that it will tend towards returning to the state of equilibrium after some perturbation by external forces. To be a bit more specific one can determine that the stability condition is given by

$$\frac{d\kappa}{d\alpha} < 0 \tag{35}$$

Where $\kappa = \frac{\bar{C}_M}{\bar{C}_L}$. To illustrate how this will control stability lets, look at Figure 7

Figure 7: Schematic of a boomerang mid flight as seen from behind

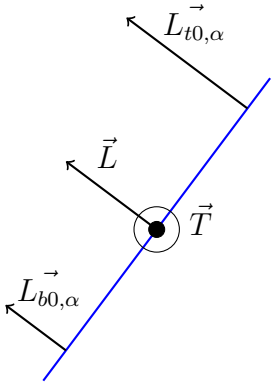

Where:

$\vec{T}$ Torque

$\vec{L}$ Angular momentum

$\vec{L_{b0,\alpha}}$ Lift force on average generated by the bottom blade

$\vec{L_{t0,\alpha}}$ Lift force on average generated by the top blade

The mass of the boomerang is not included in Figure 7 because it does not add anything to this discussion. The difference in lift force magnitude generated by the top and bottom blade is what give rise to the torque in Figure 7. Torque is the rate of change of angular momentum. As seen in the above figure, torque and angular momentum are at right angles from each other and always will be since any change in the angular momentum will result in an identical change in the orientation of the lifting forces thus in the torque. This is what give rise to the precession given by $\dot{\phi}$. This torque is also what have been mentioned as rolling moment in previous sections.
Under the assumption that a boomerang have a trim angle $\alpha = 2°$, both coefficients in 35 are positive at $\alpha = 0$(this is always the case for a positive camber air-foil) and the boomerang is thrown with $\alpha = 0$ and the slope of κ is negative this means that the coefficient of total momentum would overpower the motion thus forcing the plane of rotation to turn quicker than the lateral component of lift would turn the direction of flight. This will lead to an increasing angle of attack. If the angle is above the trim angle the opposite would be true. The precession rate would turn the plane of rotation slower than the lateral component of lift turns the direction of flight thus decreasing the angle of attack. At this point the stability

of a boomerang is explained. If we limit us to the case where $1 \leq \chi$ we can write

$$\frac{\bar{C}_M}{\bar{C}_L} = \frac{C_{l0}\left(\frac{\chi}{3}\right) + \alpha C_{l\alpha}\left(\frac{1}{4} - \frac{1}{16\chi^2}\right)}{C_{l0}\left(\frac{1}{2} + \frac{\chi^2}{3}\right) + \alpha C_{l\alpha}\left(\frac{\chi}{2} + \frac{1}{4\chi}\right)} \tag{36}$$

The above expression is a quota between two straight lines. Lets simplify a bit and introduce four labels for the coefficients. The coefficients of the straight line are as follows:

$$a = C_{l0}\left(\frac{\chi}{3}\right), \quad b = C_{l\alpha}\left(\frac{1}{4} - \frac{1}{16\chi^2}\right), \qquad c = C_{l0}\left(\frac{1}{2} + \frac{\chi^2}{3}\right), \qquad d = C_{l\alpha}\left(\frac{\chi}{2} + \frac{1}{4\chi}\right). \tag{37}$$

Performing the derivation with respect to α will yield the following result:

$$\frac{d}{d\alpha}\left(\frac{a + b\alpha}{c + d\alpha}\right) = \frac{b(c + d\alpha) - d(a + b\alpha)}{(c + d\alpha)^2} = \frac{bc - ad}{(c + d\alpha)^2}. \tag{38}$$

From this it can be seen that for a dynamically stable boomerang $ad > bc$. Expressed in χ this yields the following

$$\begin{gathered}
\left[\frac{1}{4} - \frac{1}{16\chi^2}\right]\left[\frac{1}{2} + \frac{\chi^2}{3}\right] < \left[\frac{\chi}{3}\right]\left[\frac{\chi}{2} + \frac{1}{4\chi}\right] \\
\Longleftrightarrow \\
\left[12\chi^2 - 3\right]\left[24\chi^2 + 16\chi^4\right] < \left[16\chi^3\right]\left[24\chi^3 + 12\chi\right] \\
\Longleftrightarrow \\
192\chi^6 + 240\chi^4 - 72\chi^2 < 384\chi^6 + 192\chi^4 \\
\Longleftrightarrow \\
0 < 192\chi^4 - 48\chi^2 + 72
\end{gathered} \tag{39}$$

This inequality shows when a boomerang is dynamically stable given $1 \leq \chi$, $C_{l0} > 0$ and $C_{l\alpha} > 0$. The condition $1 \leq \chi$ was used to simplify the mathematics and to present a neat result. However in [2] the author states that dynamic stability is a intrinsic property of the returning boomerang with $\chi > 0.7$.

8 Discussion and conclusion

The original idea of this paper was to add something to the study done in "Boomerang Flight Dynamics" [2]. Firstly by removing approximations made in it to see

what new information this could reveal. However these plans where abandoned when i arrived at the equations presented in 7, thereby it became abundantly clear that the simplifications where not only necessary, the information lost with those approximations where not particularly interesting for describing the stability of boomerangs. One can imagine that some information about nutation was lost, however the effect nutation would have on the stability or motion of the boomerang would clearly be a result of the average motion within one revolution anyway. The goal was changed at this point to be one where my understanding, explanation and including of omitted steps in the original was central to this paper whilst still presenting at least some of the original results. During the project my understanding of the use of the Euler angles have been greatly increased. From theory, I understood that any general rotation can be expressed as three consecutive rotations about three unique axes. Further into the project however I realised that there are natural selections of these axes that allow us to directly connects a rotational velocity to a interesting physical quantity, the zxz-convention used herein allows a straight forward connection to be made between the Euler angular velocities to rotation about the centre of mass, precession about the inertial $\hat{z}'$-axis and the rolling velocity. Another convention could result for instance in the precession speed being described by combinations of the Euler angular velocities. Lastly as some of the mathematics in the original was hard to follow I hope that they have been made clearer here.

As for the boomerang, there exists a number of preliminary conditions that must hold in order to facilitate stability. Firstly the wing tip ratio have a lower bound, $\chi > 0.7$. The air-foil needs to be designed in such a way that it generate lift at zero angle of attack. This is done by ensuring that the camber of the air-foil is positive. From the understanding of how a boomerang is stable, one can infer what could possibly be done to make the boomerang more stable and also how to make the radius of flight designable. By increasing the camber one can increase the lift at zero angle of attack, this should result in a faster convergence toward the trim state. By increasing the trim state angle the radius of flight might be reduced. This conclusion is however uncertain in the context of this work since we assume small angles, α. A last point about design, if the boomerang is made thinner whilst maintaining the same amount of camber the radius of flight should reduce. This is due to the consequent reduction in inertial mass and moment. Improvements to the model made herein and in [2] will include but would not be limited to, a more accurate description of the angle of attack dependence of the coefficients, allowing for 3-dimensional airflow in the BET and use actual mass properties of a boomerang.

As a concluding statement I would like to say that the dynamics of boomerangs are an immensely interesting topic with a lot of lessons to teach in both mechanics

and aerodynamics. Even after significant simplifications something can be said about the stability of flight and by understanding how the boomerang is stable we can venture some guesses about design characteristics that might alter or improve the boomerang.

References

[1] (Jan. 2018), [Online]. Available: http://www.4physics.com/catalog/images/LHBoomerangMeasure.png.

[2] J. Vassberg, "Boomerang flight dynamics", in *30th AIAA Applied Aerodynamics Conference*, 2012, p. 2650.

[3] (2017), [Online]. Available: http://www.aerochapter.com/notes.php?name=Module%208&inst=1&nid=6&top=15&tit=15&subj=EASA%20Modules.

[4] (2018), [Online]. Available: https://en.wikipedia.org/wiki/Coand%C4%83_effect.

[5] (2017), [Online]. Available: https://en.wikipedia.org/wiki/Blade_element_theory.